ACS Medicinal Chemistry Letters

pubs.acs.org/acsmedchemlett

Structures of 1-Deoxy-D-Xylulose-5-Phosphate Reductoisomerase/Lipophilic Phosphonate Complexes

Lisheng Deng,[†] Kiwamu Endo,[‡] Masahiro Kato,[‡] Gang Cheng,[†] Shunsuke Yajima,*[,‡] and Yongcheng Song*[,†]

[†]Department of Pharmacology, Baylor College of Medicine, 1 Baylor Plaza, Houston, Texas 77030, United States, and
[‡]Department of Bioscience, Tokyo University of Agriculture, Setagaya-ku, Tokyo 156-8502, Japan

ABSTRACT Fosmidomycin, a potent inhibitor of 1-deoxy-D-xylulose-5-phosphate reductoisomerase (DXR), has antibacterial and antimalaria activity. Due to its poor pharmacokinetics, more lipophilic DXR inhibitors are needed. However, the hydrophobic binding site(s) in DXR remains elusive. Here, pyridine/quinoline containing phosphonates are identified to be DXR inhibitors with IC_{50} values as low as 840 nM. We also report three DXR/inhibitor structures, revealing a novel binding mode. The indole group of Trp211 is found to move ~4.6 Å to open up a mainly hydrophobic pocket, where the pyridine/quinoline rings of the inhibitors are located and have strong $\pi-\pi$ stacking/charge-transfer interactions with the indole. Docking studies demonstrate our structures could be used to predict the binding modes of other lipophilic DXR inhibitors. Overall, this work shows an important role of Trp211 in inhibitor recognition and provides a structural basis for future drug design and development.

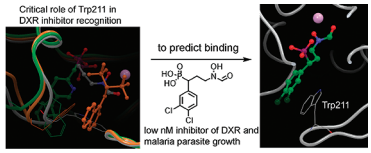

KEYWORDS 1-Deoxy-D-xylulose-5-phosphate reductoisomerase, protein crystallography, anti-infective, drug design, inhibitor recognition

The second enzyme in the methylerythritol phosphate (MEP) isoprene biosynthesis pathway (Supporting Information Figure S1) used by malaria parasite and most bacteria, 1-deoxy-D-xylulose-5-phosphate reductoisomerase (DXR), is a validated anti-infective drug target.[1,2] DXR catalyzes the conversion of 1-deoxy-D-xylulose-5-phosphate (DXP) to 2-*C*-methyl-D-erythritol-4-phosphate (MEP) with a Mg^{2+} and NADPH being the enzyme cofactors. Fosmidomycin (**1**, Chart 1) is a potent DXR inhibitor[3] and has antibacterial and antimalaria activity in preclinical studies and clinical trials.[4−6] However, due to its high hydrophilicity, **1** exhibits a short half-life (~1 h) in plasma and poor oral availability. In addition, since **1** is actively transported into cells via glycerol-3-phosphate transporter GlpT,[7] pathogens without GlpT, such as Gram-positive bacteria, are resistant to **1** due to limited cellular uptake.[8] Great interest has therefore been generated to develop potent inhibitors of DXR.[9−20]

The central theme for the development is to find potent, more lipophilic inhibitors that might possess improved pharmacokinetic properties. Medicinal chemistry based on **1** has been investigated for the past decade.[9−18] Although most of these modifications yielded compounds with considerably reduced activity, compounds **3**−**8** bearing an α-substituent largely maintain the inhibitory activity.[9] The best compound is **8** with a 3,4-dichlorophenyl group having a similar enzyme activity as that of **1**. However, **8** demonstrated > 10× increased activity against the malaria parasite *Plasmodium falciparum* (EC_{50} of 90 nM vs 1.1 μM for **1**), presumably due to enhanced cellular uptake. Other lipophilic inhibitors **3**−**7** also exhibited better antimalaria activity (EC_{50}'s of 0.25−0.95 μM) than **1**. Structure activity relationship (SAR) analysis of **3**−**7** revealed that DXR inhibition appears to be correlated to the increased electron-deficiency of their phenyl rings.[9] However, the underlying mechanism remains unknown. DXR inhibitors that are structurally distinct from **1** are scarce. The two bisphosphonates **9** and **10** were found to be relatively weak inhibitors (IC_{50} = 4 and 7 μM).[19] We recently used a coordination chemistry based design to find a lipophilic inhibitor **11** (IC_{50} = 1.4 μM) with a broad antibacterial activity.[20]

It is of interest to investigate how lipophilic inhibitors **3**−**8** bind to DXR, especially with respect to the binding site of their hydrophobic groups. The structural probing should facilitate further inhibitor design and development for antibacterial and antimalaria purposes, since these widespread, drug-resistant pathogens kill millions of people each year worldwide. However, their X-ray structures in complex with DXR are not available. In fact, only two types of DXR/inhibitor structures have been reported, i.e., DXR with **1**[21−24] and bisphosphonates **9** and **10**.[19]

Received Date: October 7, 2010
Accepted Date: November 15, 2010
Published on Web Date: November 24, 2010

DOI: 10.1021/ml100243r | *ACS Med. Chem. Lett.* **2011**, *2*, 165–170

Chart 1. Structures of Known DXR Inhibitors **1**−**11**, Together with Their IC_{50} Values against *E. coli* DXR in Parentheses (IC_{50} Values Are from the Original Refs 9, 19, and 20)

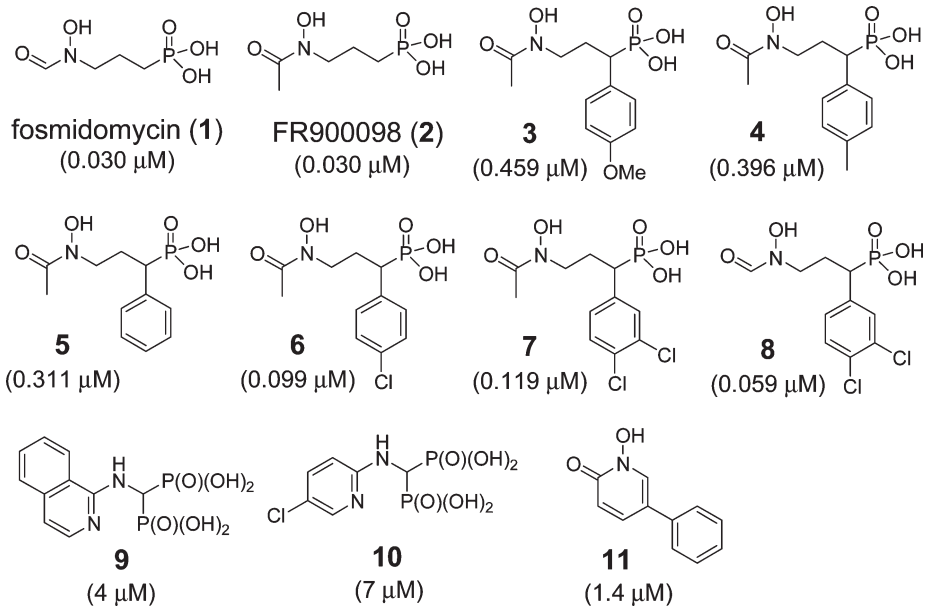

Chart 2. Structures of **12**−**19**, Together with Their IC_{50} Values against *E. coli* DXR in Parentheses

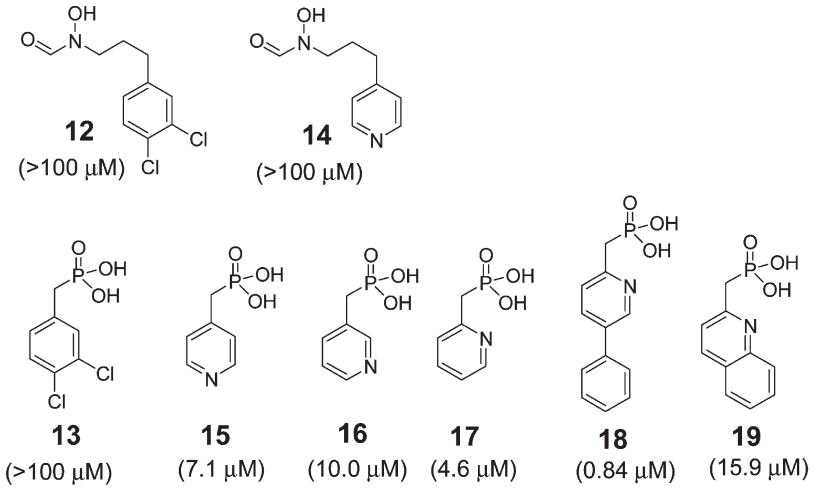

To find lipophilic analogues of **8** that are active against DXR, we synthesized compounds **12** and **13** (Chart 2 and Supporting Information Experimental Section). These two compounds were designed by removing either the phosphonate group (for **12**) or the hydroxamate moiety (for **13**) from **8**. However, when tested against recombinant *E. coli* DXR, both compounds were found to have no activity at 100 μM. Since SAR suggested a more electron-deficient ring could be favored,[9] **14** and **15** with a pyridin-4-yl group were prepared. Although hydroxamate **14** is not active, compound **15** was found to be a DXR inhibitor with an IC_{50} value of 7.1 μM. Analogous **16** and **17** with a pyridin-3-yl and -2-yl side chain were subsequently made and found to be also active, with **17** having an IC_{50} value of 4.6 μM. To further probe the hydrophobic feature of DXR, more lipophilic **18** and **19** were synthesized. **18**, 5-phenylpyridin-2-ylmethylphosphonic acid, exhibits the strongest DXR inhibition in this series (IC_{50} = 0.84 μM). **19**, having a quinolin-2-yl group, is weaker than **17** (IC_{50} = 15.9 μM). Compounds **15**−**19** represent a new class of lipophilic DXR inhibitors that are structurally distinct from **1**, with **18** being among the very few inhibitors possessing submicromolar activity. These compounds should provide a new scaffold for further inhibitor development. Moreover, they can be exploited to probe the elusive hydrophobic pocket(s) of DXR.

We performed X-ray crystallographic studies and obtained the crystal structures of **17**−**19** complexed with *E. coli* DXR. The structures were refined at 2.1 Å (for DXR/**17**) or 2.0 Å (for DXR/**18** and DXR/**19**) with the crystallographic details and overall structures shown in Table S1 and Figures S2. The three protein complexes crystallize as homodimers, with

DOI: 10.1021/ml100243r | *ACS Med. Chem. Lett.* **2011**, *2*, 165–170

each subunit containing one inhibitor and one NADPH molecule. Their overall 3-D structures are similar to those previously reported.[19,21−24] As shown in Figure 1a, **17**−**19** bind to the same site as **1** and DXP, showing a competitive mode of action. The phosphonate groups of our inhibitors are located in the phosphonate binding site of **1**. The distances between the P atoms of **17**−**19** and that of **1** are ∼1.3 Å. Each of the electron-deficient pyridine/quinoline rings has a $\pi-\pi$ stacking interaction with the electron-rich indole ring of Trp211, with the distance between the two parallel rings being ∼3.5 Å (Figure 1B−D). Possible charge-transfer makes the interaction particularly strong, which could elucidate why **15**−**19** have good inhibitory activity,

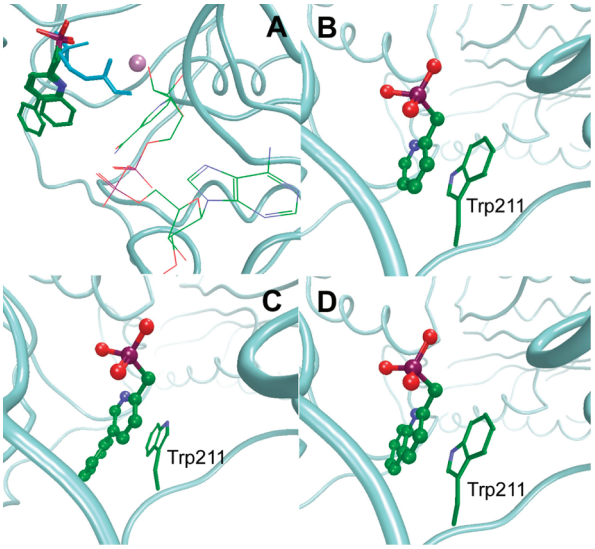

Figure 1. (A) Superimposed structures of **17**−**19** and **1** (in cyan) in DXR with NADPH; (B) active site of the DXR/**17** complex; (C) active site of the DXR/**18** complex; (D) active site of the DXR/**19** complex.

while **13** is inactive. The hydroxamate binding site of **1** is unoccupied. Moreover, there is no Mg^{2+} observed, despite 5 mM of Mg^{2+} present in the crystallization buffer. This could be due to the acidic crystallization condition (pH = 5.6) leading to a higher K_m (17 mM) for Mg^{2+}.[23] It is remarkable that three carboxylates of metal binding residues Asp149, Glu151, and Glu230 are still positioned very close to those with a bound Mg^{2+} in the DXR/**1** complex (Figure S3).

The overall 3-D structures of the DXR/**17**−**19** complexes are almost identical (Figure 2a). However, the conformation of Trp211 in the DXR/**18** complex is different, with the indole ring flipped almost 180° (Figure 1B−D). This orientation could allow the 5-phenylpyridine group of **18** to have more $\pi-\pi$ stacking and hydrophobic interactions with the indole, which might account for the enhanced activity of **18**. We next examined functions of Trp211 in other DXR/inhibitor complexes. As shown in Figure 2b, superposition of the DXR/**1**,[24] DXR/**9**,[19] and DXR/**18** structures shows major conformational changes for a flexible loop containing residues 205−215 in the DXR active site, while only subtle deviations are observed for the remaining part of the protein backbone. Even more noticeable is the conformational change of the Trp211 indole ring (Figure 2c). In the DXR/**1** structure, the indole ring moves toward the center of the active site and covers the top of the carbon skeleton of **1**, which is relatively hydrophobic. This allows the hydrophobic indole group to separate **1** from the solvent and largely close the active site, which might account for its tight binding. The structures of DXR complexed with **18** and **9** demonstrate the flexible loop has great plasticity such that the Trp211 indole ring is able to move considerably in order to have favorable interactions with the lipophilic groups of these inhibitors (Figure 2c). The indole N atoms of the DXR/**18** and DXR/**9** complexes are 4.6 Å and 4.4 Å away from that of the DXR/**1** complex, respectively. In the DXR/bisphosphonate complexes, the indole could also possess $\pi-\pi$ stacking/charge transfer interactions with the isoquinoline (for **9**) or pyridine ring

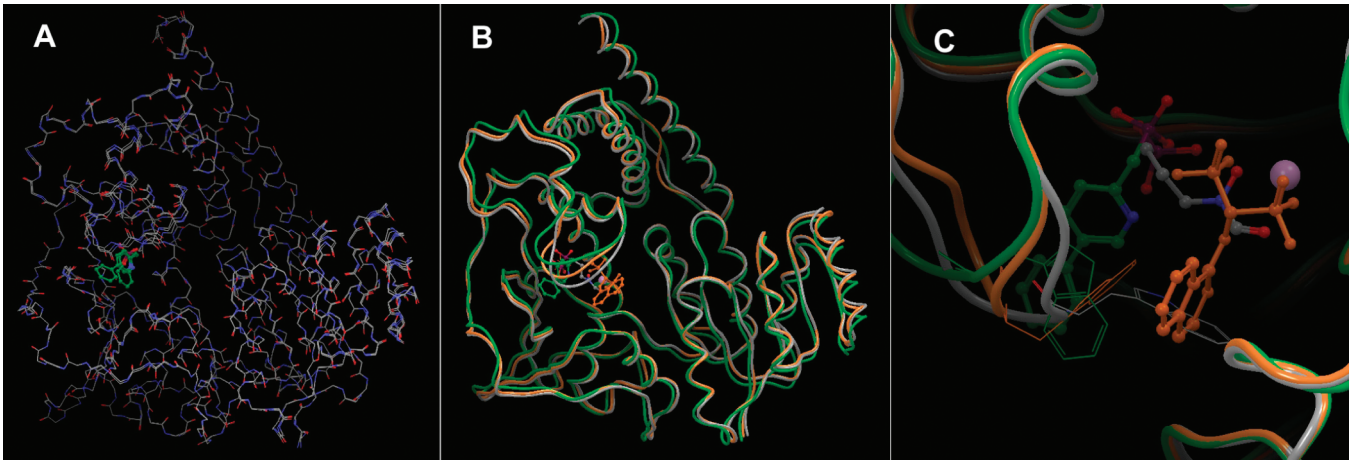

Figure 2. (A) Protein backbones of the superimposed structures of the DXR/**17**−**19** complexes; (B) tube models of the superimposed structures of the DXR/**18** (in green), DXR/**1** (in gray), and DXR/**9** (in orange) complexes, showing major conformational changes for the flexible loop in the active site; (C) close-up view of the superimposed active sites of the DXR/**18** (in green), DXR/**1** (in gray), and DXR/**9** (in orange) complexes, showing the indole ring of Trp211 moves considerably to recognize different inhibitors bound to DXR. Mg^{2+} is shown as a pink sphere.

DOI: 10.1021/ml100243r | ACS Med. Chem. Lett. 2011, 2, 165–170

(for **10**), although there is a small angle of ~15° between the two rings.

It is clear that Trp211 plays an important role in recognizing all of the DXR inhibitors with known structures, which suggests that an electron-deficient, hydrophobic group could be favored for future inhibitor design. Moreover, Trp211 is conserved across the species using the MEP pathway (Figure S4). It is therefore likely that inhibitors having strong interactions with Trp211 could exhibit broad activity.

The crystal structures of the DXR/**17**−**19** complexes reveal two mainly hydrophobic pockets. The conformational change of Trp211 opens up a large, mainly hydrophobic pocket (pocket A), defined by Trp211, Pro273, His208, His256, Asn210, Ser253, and Ser150. In the previously reported structures, the corresponding pocket A is largely compressed due to the orientation of the Trp211 side chain and, thus, poorly defined. Pocket B is surrounded by the residues Trp211, Met 213, Met275, and Ser150, which is not occupied by **17**−**19**. Rather, this pocket is the binding site of the hydrophobic groups of **9** and **10**.

We finally investigated if our structures with newly discovered pocket A could be used to model the binding structures of **3**−**8**, using Glide in the Schrödinger Suite.[25] First, we found Glide is able to well predict the binding modes of **1**, **10**, and **17**, with each set of 10 docking structures with lowest energies having rms (root-mean-square) deviations of 0.37−1.9 Å (Figure S5). We next used the DXR/**17** structure to model the binding mode of **8**. Since a Mg^{2+} is needed for successful docking of **8** having a hydroxamate group, Mg^{2+} was extracted from DXR/**1** and added into DXR/**17**, and the new structure was energy-minimized. This is reasonable, as the conformations of Mg^{2+}-binding residues Asp149, Glu151, and Glu230 do not change significantly (Figure S3). Since **8** contains an asymmetric α-carbon atom, both enantiomers (*R*)- and (*S*)-**8** were docked into the DXR/**17** structure with the Mg^{2+} and the results shown in Figure 3A−C. (*R*)-**8** can be docked favorably, with 10 tightly clustered docking structures mimicking the binding mode of **1**. All of the phosphonate groups are located in the phosphonate binding site of **1**, and each of the hydroxamate moieties chelates Mg^{2+}, which is the "gold" standard for docking a hydroxamate into a metalloenzyme. In addition, all of the 3,4-dichlorophenyl groups occupy pocket A and have $\pi-\pi$ stacking interactions with the Trp211 indole ring. However, docking (*S*)-**8** yielded a relatively poor result (Figure 3c). All of the 10 docking structures show a "reversed" binding mode with the phosphonate binding to Mg^{2+} and the hydroxamate located in the phosphonate binding site. In addition, their 3,4-dichlorophenyl groups are in pocket B without interactions with Trp211.

Docking studies of **8** using the DXR/**1** and DXR/**10** structures were also performed as a comparison. In both cases, (*R*)- and (*S*)-**8** are predicted to adopt a "reversed" binding style (Figure S6), with all of the phosphonate groups binding to Mg^{2+}. The hydroxamate groups are mostly located in the phosphonate binding site and the lipophilic 3,4-dichlorophenyl group found in Pocket B. These results show our DXR structures could be a better platform for modeling compound **8**. Interestingly, these results also suggest that (*R*)-**8** might have better activity than its (*S*)-enantiomer, which is also implied by superimposing DXR/**1** to DXR/**17** (Figure 1a). Should the pyridin-2-yl group have been attached to the α-position of **1**, the virtually generated molecule would have a *R*-configuration.

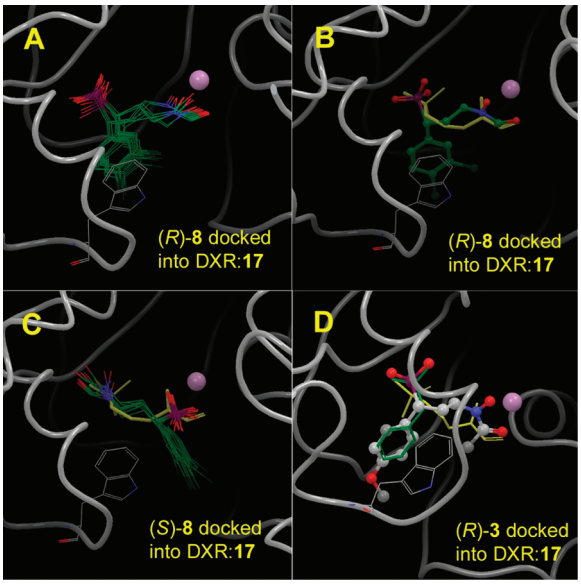

Figure 3. (A) Docking result of (*R*)-**8** using the DXR/**17** structure with a Mg^{2+} (pink sphere); (B) lowest energy docking structure of (*R*)-**8**, superimposed with **1** (in yellow), showing (*R*)-**8** is predicted to bind favorably to DXR; (C) docking result of (*S*)-**8** using the DXR/**17** structure, exhibiting a "reversed" binding mode; (D) lowest-energy docking structure of (*R*)-**3** using the DXR/**17** structure, superimposed with the crystal structures of **1** (in yellow) and **17** (in green).

Docking studies of compounds **3**−**7** yielded similar outcomes. The (*R*)-enantiomers can be docked favorably into our DXR structures (Figures 3d and S7). It is noteworthy that these docking results are supported by previously reported SAR of **3**−**7**.[9] The generally increasing activities from **3** to **7** (4-OMe-Ph < 4-Me-Ph < H−Ph < 4-Cl-Ph ≈ 3,4-diCl-Ph) are correlated to their interactions with the electron-rich Trp211 indole ring. Our crystallographic and modeling studies now provide a structural basis to validate these experimental data.

In summary, this work is of interest for a number of reasons. First, potent lipophilic DXR inhibitors are needed for their potential to become new drugs to treat drug-resistant bacterial and malarial infections. However, structural insight into the hydrophobic nature of the DXR active site remains unclear. We have found pyridine/quinoline containing phosphonates **15**−**19** to be a new class of DXR inhibitors (IC_{50}'s as low as 0.84 μM). Second, we solved the structures of three DXR/inhibitor complexes that reveal a novel inhibitor binding mode. Of particular interest is that the conformation of the flexible loop is changed considerably, with the Trp211 indole ring moving ~4.6 Å to open up a large, mainly hydrophobic pocket. The pyridine/quinoline rings are located in this newly formed cavity and have $\pi-\pi$ stacking/charge-transfer interactions with the indole. Analysis of all DXR/inhibitor structures uncovers the critical role

DOI: 10.1021/ml100243r | ACS Med. Chem. Lett. 2011, 2, 165–170

of Trp211 in inhibitor recognition and binding. Third, docking studies show our structures could be a better platform for modeling the binding modes of **3**−**8**, supported by SAR of these inhibitors. Overall, this work provides a structural basis for future design and development of lipophilic DXR inhibitors.

SUPPORTING INFORMATION AVAILABLE Figures showing the methylerythritol phosphate (MEP) isoprene biosynthesis pathway, the structures of DXR/**17**, DXR/**18**, and DXR/**19**, ClustalX alignment of DXRs, and docking structures of **1**, **4**−**8**, and **10**; table of data collection and refinement statistics; and an Experimental Section giving synthesis and compound analysis details. This material is available free of charge via the Internet at http://pubs.acs.org.

Accession Codes: The coordinates for the DXR/**17**, DXR/**18**, and DXR/**19** complexes have been deposited in the Protein Data Bank as entries 3ANL, 3ANM, and 3ANN, respectively.

AUTHOR INFORMATION

Corresponding Author: *To whom correspondence should be addressed. Telephone: +81 (3) 5477-2768. E-mail: yshun@nodai.ac.jp (S.Y.). Telephone: 713-798-7415. E-mail: ysong@bcm.edu (Y.S.).

Author Contributions: L.D. performed inhibitor synthesis and analyzed data; K.E. and M.K. did protein production and crystallization; S.Y. designed crystallographic studies and performed data collection and structure refinement; G.C. analyzed data; and Y.S. designed the research, carried out enzyme assay and molecular modeling and wrote the paper.

ACKNOWLEDGMENT This work was supported by a grant (R21AI088123) from the National Institute of Allergy and Infectious Diseases to Y.S. and in part by Grants-in-aids for Scientific Research 19580396 from the Ministry of Education, Science, Sports, and Culture of Japan to S.Y. We thank the staff of the Photon Factory for assistance in data collection.

ABBREVIATIONS DXR, 1-deoxy-D-xylulose-5-phosphate reductoisomerase; DXP, 1-deoxy-D-xylulose-5-phosphate; IPP, isopentenyl diphosphate; DMAPP, dimethylallyl diphosphate; MEP, 2-*C*-methyl-D-erythritol-4-phosphate; SAR, structure activity relationship.

REFERENCES

(1) Hunter, W. N. The non-mevalonate pathway of isoprenoid precursor biosynthesis. *J. Biol. Chem.* **2007,** *282*, 21573–21577.
(2) Testa, C. A.; Brown, M. J. The methylerythritol phosphate pathway and its significance as a novel drug target. *Curr. Pharm. Biotechnol.* **2003,** *4*, 248–259.
(3) Kuzuyama, T.; Shimizu, T.; Takahashi, S.; Seto, H. Fosmidomycin, a specific inhibitor of 1-deoxy-D-xylulose 5-phosphate reductoisomerase in the nonmevalonate pathway for terpenoid biosynthesis. *Tetrahedron Lett.* **1998,** *39*, 7913–7916.
(4) Mine, Y.; Kamimura, T.; Nonoyama, S.; Nishida, M.; Goto, S.; Kuwahara, S. *In vitro* and *in vivo* antibacterial activities of FR-31564, a new phosphonic acid antibiotic. *J. Antibiot.* (*Tokyo*) **1980,** *33*, 36–43.
(5) Jomaa, H.; Wiesner, J.; Sanderbrand, S.; Altincicek, B.; Weidemeyer, C.; Hintz, M.; Turbachova, I.; Eberl, M.; Zeidler, J.; Lichtenthaler, H. K.; Soldati, D.; Beck, E. Inhibitors of the nonmevalonate pathway of isoprenoid biosynthesis as antimalarial drugs. *Science* **1999,** *285*, 1573–1576.
(6) Missinou, M. A.; Borrmann, S.; Schindler, A.; Issifou, S.; Adegnika, A. A.; Matsiegui, P. B.; Binder, R.; Lell, B.; Wiesner, J.; Baranek, T.; Jomaa, H.; Kremsner, P. G. Fosmidomycin for malaria. *Lancet* **2002,** *360*, 1941–1942.
(7) Sakamoto, Y.; Furukawa, S.; Ogihara, H.; Yamasaki, M. Fosmidomycin resistance in adenylate cyclase deficient (*cya*) mutants of *Escherichia Coli*. *Biosci. Biotechnol. Biochem.* **2003,** *67*, 2030–2033.
(8) Dhiman, R. K.; Schaeffer, M. L.; Bailey, A. M.; Testa, C. A.; Scherman, H.; Crick, D. C. 1-Deoxy-D-xylulose 5-phosphate reductoisomerase (IspC) from *Mycobacterium tuberculosis:* towards understanding mycobacterial resistance to fosmidomycin. *J. Bacteriol.* **2005,** *187*, 8395–8402.
(9) Haemers, T.; Wiesner, J.; Van Poecke, S.; Goeman, J.; Henschker, D.; Beck, E.; Jomaa, H.; Van Calenbergh, S. Synthesis of α-substituted fosmidomycin analogues as highly potent *Plasmodium falciparum* growth inhibitors. *Bioorg. Med. Chem. Lett.* **2006,** *16*, 1888–1891.
(10) Devreux, V.; Wiesner, J.; Jomaa, H.; Rozenski, J.; Van der Eycken, J.; Van Calenbergh, S. Divergent strategy for the synthesis of α-aryl-substituted fosmidomycin analogues. *J. Org. Chem.* **2007,** *72*, 3783–3789.
(11) Shtannikov, A. V.; Sergeeva, E. E.; Biketov, S. F.; Ostrovskii, D. N. Evaluation of *in vitro* antibacterial activity of fosmidomycin and its derivatives. *Antibiot. Khimioter.* **2007,** *52*, 3–9.
(12) Kuntz, L.; Tritsch, D.; Grosdemange-Billiard, C.; Hemmerlin, A.; Willem, A.; Bach, T. J.; Rohmer, M. Isoprenoid biosynthesis as a target for antibacterial and antiparasitic drugs: phosphonohydroxamic acids as inhibitors of deoxyxylulose phosphate reducto-isomerase. *Biochem. J.* **2005,** *386*, 127–135.
(13) Merckle, L.; Andres-Gomez, A.; Dick, B.; Cox, R. J.; Godfrey, C. R. A fragment-based approach to understanding inhibition of 1-deoxy-D-xylulose-5-phosphate reductoisomerase. *ChemBioChem* **2005,** *6*, 1866–1874.
(14) Munos, J. W.; Pu, X.; Liu, H. W. Synthesis and analysis of a fluorinated product analogue as an inhibitor for 1-deoxy-D-xylulose 5-phosphate reductoisomerase. *Bioorg. Med. Chem. Lett.* **2008,** *18*, 3090–3094.
(15) Ortmann, R.; Wiesner, J.; Silber, K.; Klebe, G.; Jomaa, H.; Schlitzer, M. Novel deoxyxylulosephosphate-reductoisomerase inhibitors: fosmidomycin derivatives with spacious acyl residues. *Arch. Pharm.* (*Weinheim*) **2007,** *340*, 483–490.
(16) Silber, K.; Heidler, P.; Kurz, T.; Klebe, G. AFMoC enhances predictivity of 3D QSAR: a case study with DOXP-reductoisomerase. *J. Med. Chem.* **2005,** *48*, 3547–3563.
(17) Woo, Y. H.; Fernandes, R. P.; Proteau, P. J. Evaluation of fosmidomycin analogs as inhibitors of the *Synechocystis sp.* PCC6803 1-deoxy-D-xylulose 5-phosphate reductoisomerase. *Bioorg. Med. Chem.* **2006,** *14*, 2375–2385.
(18) Kurz, T.; Schlüter, K.; Kaula, U.; Bergmann, B.; Walter, R. D.; Geffken, D. Synthesis and antimalarial activity of chain substituted pivaloyloxymethyl ester analogues of Fosmidomycin and FR900098. *Bioorg. Med. Chem.* **2006,** *14*, 5121–5135.
(19) Yajima, S.; Hara, K.; Sanders, J. M.; Yin, F.; Ohsawa, K.; Wiesner, J.; Jomaa, H.; Oldfield, E. Crystallographic structures of two bisphosphonate:1-deoxyxylulose-5-phosphate reductoisomerase complexes. *J. Am. Chem. Soc.* **2004,** *126*, 10824–10825.

DOI: 10.1021/ml100243r | *ACS Med. Chem. Lett.* **2011**, *2*, 165–170

(20) Deng, L.; Sundriyal, S.; Rubio, V.; Shi, Z.; Song, Y. Coordination Chemistry Based Approach to Lipophilic Inhibitors of 1-Deoxy-D-xylulose-5-phosphate Reductoisomerase. *J. Med. Chem.* **2009,** *52*, 6539–6542.
(21) Yajima, S.; Nonaka, T.; Kuzuyama, T.; Seto, H.; Ohsawa, K. Crystal structure of 1-deoxy-D-xylulose 5-phosphate reductoisomerase complexed with cofactors: implications of a flexible loop movement upon substrate binding. *J. Biochem.* **2002,** *131*, 313–317.
(22) Steinbacher, S.; Kaiser, J.; Eisenreich, W.; Huber, R.; Bacher, A.; Rohdich, F. Structural basis of fosmidomycin action revealed by the complex with 2-C-methyl-D-erythritol 4-phosphate synthase (IspC). Implications for the catalytic mechanism and anti-malaria drug development. *J. Biol. Chem.* **2003,** *278*, 18401–18407.
(23) Mac Sweeney, A.; Lange, R.; Fernandes, R. P.; Schulz, H.; Dale, G. E.; Douangamath, A.; Proteau, P. J.; Oefner, C. The crystal structure of *E.coli* 1-deoxy-D-xylulose-5-phosphate reductoisomerase in a ternary complex with the antimalarial compound fosmidomycin and NADPH reveals a tight-binding closed enzyme conformation. *J. Mol. Biol.* **2005,** *345*, 115–127.
(24) Yajima, S.; Hara, K.; Iino, D.; Sasaki, Y.; Kuzuyama, T.; Ohsawa, K.; Seto, H. Structure of 1-deoxy-D-xylulose 5-phosphate reductoisomerase in a quaternary complex with a magnesium ion, NADPH and the antimalarial drug fosmidomycin. *Acta Crystallogr., Sect. F: Struct. Biol. Cryst. Commun.* **2007,** *63*, 466–470.
(25) Glide, version 5.5; Schrödinger, LLC: New York, NY, 2009. Schrödinger Suite 2009; Schrödinger, LLC: New York, NY, 2009.

DOI: 10.1021/ml100243r | *ACS Med. Chem. Lett.* **2011**, *2*, 165–170